Design and Potential of EMI CM Chokes with Integrated DM Inductance

Mohammad Ali, Rehnuma Bushra, Jens Friebe, Axel Mertens
LEIBNIZ UNIVERSITY HANNOVER
Institute for Drive Systems and Power Electronics
Welfengarten 1
30167 Hannover, Germany
Tel: +49 / (0) - 511 762 3778
Fax: +49 / (0) - 511 762 3040
E-mail: mohammad.ali@ial.uni-hannover.de
URL: www.ial.uni-hannover.de

Acknowledgments

This work was supported by Forschungsvereinigung Antriebstechnik e.V. (FVA) within Project FVA 637V.

Keywords

≪Choke≫, ≪3-D Electromagnetic Modeling≫, ≪DM Inductance≫,≪Electromagnetic Interference (EMI) Filters≫, ≪Mutual Couplings≫, ≪Filter Optimization≫.

Abstract

A common-mode (CM) choke is one of the major filtering components used in electromagnetic interference (EMI) filters that impede the flow of common-mode current in the system. Besides, a common-mode choke also offers a finite differential-mode (DM) inductance in the form of leakage inductance. In general, the leakage inductance is small, which necessitates extra DM inductors and leads to a large filter size. In this paper, a single-phase CM choke is designed with an integrated DM inductance for use in EMI filters, based on a flux bypass inside the toroidal core. The DM inductance of these chokes can be altered by redesigning the windings, while the CM inductance remains identical to a conventional CM choke. The design and effectiveness of them are further supported by theoretical, simulated, and measurement results and core saturation analysis. Finally, an extension to three-phase CM chokes with integrated three-phase DM inductance is discussed.

I. Introduction

The introduction of wide-bandgap power semiconductors has made EMI filter design quite challenging when aiming to meet the EMC regulations according to IEC and CISPR standards. EMI filters have to attenuate high emission levels, especially at higher frequencies in the MHz range generated from the steep $\frac{\mathrm{d}v}{\mathrm{d}t}$ switching rate of the wide-bandgap power semiconductor devices. An EMI filter usually attenuates both common-mode (CM) and differential-mode (DM) noise. A common-mode (CM) choke is an indispensable part of an EMI filter that helps to attenuate the CM noise between the phase and neutral lines with reference to the ground. The CM choke typically consists of a soft magnetic toroidal core with windings wound around the core. It usually provides a large CM inductance. For fixed core dimensions, the CM inductance is directly proportional to the square of the number of turns in each winding. However, as $100\,\%$ coupling does not occur between the windings of the CM choke, leakage inductance exists in the operation of a conventional CM choke. This leakage inductance acts like the DM inductance and suppresses the DM noise between the phase and neutral lines. In most cases, however, the leakage inductance of a choke is not sufficient to suppress the DM noise [1], [2], [3], [4]. To improve the DM performance, a single-phase common-mode choke usually uses two additional external inductors, which result in a larger filter. Therefore, a CM choke with an integrated DM inductor can be the solution when trying to reduce the size of the inductor of an EMI filter and improve the DM attenuation [5], [6]. According to [5], an integrated DM inductor with a conventional CM choke may reduce an EMI filter's volume up to $30\,\%$.

However, most of the literature on common-mode chokes does not address how to improve the DM inductance. Only limited literature especially analyzes the improvement of the DM inductance of a common-mode choke [5], [7], [8]. In [9], [10], an asymmetric winding structure is proposed to attenuate DM noise along with the CM noise. However, an asymmetric winding structure may create radiated emissions at higher frequencies and requires careful analysis with respect to core saturation. In [5], a new core structure consisting of two cores, a toroidal core, and a solenoid core, is proposed. However, the effect of different parameters on the performance of the new choke is not clearly discussed. This paper shows the effect of different parameters (number of turns on the block core, air-gap effect, relative permeability, and core material effect) on the performance of a conventional CM choke with a block core and its attenuation in an EMI filter. In addition, a new choke structure with a Y-core to improve the DM inductance of a three-phase CM choke is also proposed in this paper.

II. Winding Structures to Improve DM Inductance

A. Structure of a Single-Phase CM Choke with Block Core

Fig. 1 shows a single-phase CM choke with a block core and its simulation model. After inserting the block core, the DM inductance of the respective choke can be further improved by introducing a number of turns on the block core. There are six independent copper windings on the cores: four on the toroidal core ($T_1\prime$, $T_1\prime\prime$, $T_2\prime$, $T_2\prime\prime$), and two on the block core (B_1, B_2), as indicated in Figs. 1e and 1f [5]. The coils $T_1\prime$, B_1, $T_1\prime\prime$ and $T_2\prime$, B_2, $T_2\prime\prime$ each comprise two separate windings of this single-phase CM choke. The four windings on the toroidal core have the same number of turns, and the two windings on the block core also have an identical number of turns to ensure a symmetrical and homogeneous structure.

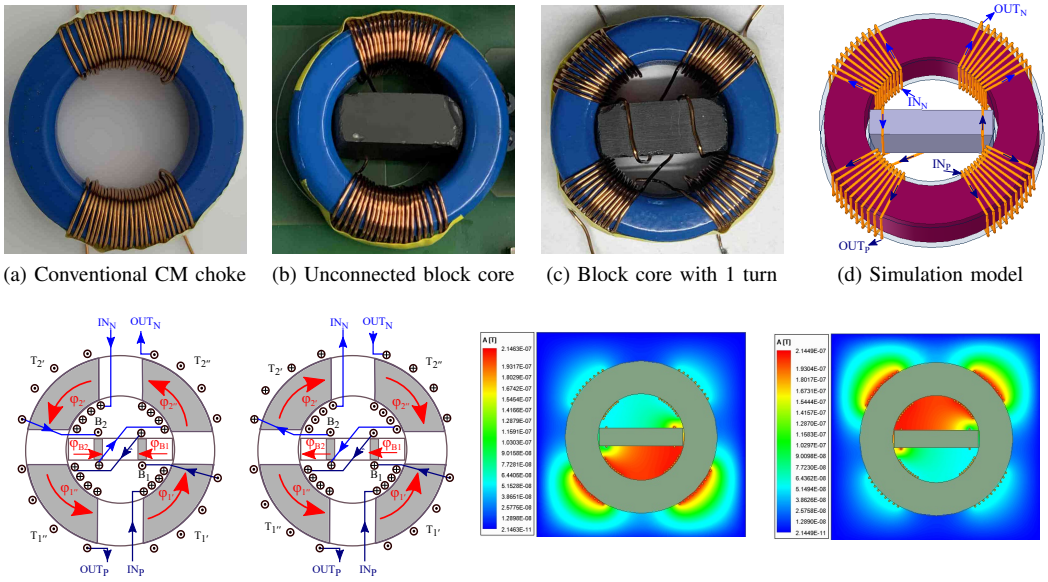

(a) Conventional CM choke (b) Unconnected block core (c) Block core with 1 turn (d) Simulation model

(e) CM flux direction (f) DM flux direction (g) Magnetic flux distribution (h) Magnetic flux distribution

Fig. 1. Single-phase CM choke: (a) conventional CM choke; (b) CM choke with unconnected block core; (c) CM choke with 1 turn in block core; (d) Q3D simulation model; (e) CM flux direction; (f) DM flux direction; (g) Magnetic flux distribution (winding 1); (h) Magnetic flux distribution (winding 2)

The flux direction in this new choke is shown in Figs. 1e and 1f. The red arrows in the figure show the magnetic flux direction, and the light blue and dark blue arrows indicate the current direction in the choke. Current entering the plane of the diagram is indicated by the circled cross and current exiting the plane is indicated by the circled dot. In determining the direction of the flux, it is assumed that the current flows from the cross to the dot. As shown in Fig. 1e, the flux induced by the CM current is oriented anticlockwise, and for the two windings on the toroidal, the fluxes add together to provide high CM inductance, as in a conventional CM choke. However, because of the opposite induced flux in the block core, the two fluxes oppose each other without significantly affecting the CM inductance of the choke. On the one hand, the directions of the magnetic fluxes created by the DM current in the toroidal core exactly oppose each other, as shown in Fig. 1f. In addition, the windings on the block core create two fluxes with the same direction and produce more magnetic flux inside the core, thus resulting in more leakage flux in the air gap between the toroidal and block core. For the magnetic flux density analysis, a simulation model was developed in ANSYS Q3D, as shown in Fig. 1d. The distribution of magnetic flux in the CM choke with the block core is shown in Figs. 1g and 1h. These figures show higher magnetic flux distribution in the inner portion of the toroidal core due to the block core and increased leakage inductance along the magnetic path created by the block core. As a result, a high DM inductance can be obtained from this configuration.

B. Magnetic and Electrical Circuits of a Single-Phase CM Choke with a Block Core

Magnetic circuits are primarily concerned with the behavior of magnetic fields within a single component or a group of components. Therefore, it is quite easy to obtain the electrical circuit of an electromagnetic component, e.g., an inductor, from the magnetic circuit. In the magnetic circuit, the magnetomotive force (MMF) is represented by NI, where N denotes the number of turns in the winding, and I represents the current flowing through it. The polarity of the MMF is determined by the flux direction. In the magnetic circuit, $\mathfrak{R}_\mathrm{T}$, $\mathfrak{R}_\mathrm{B}$ denote the reluctance of the toroidal core and block core, respectively. The reluctance of the air gap between the block core and the toroidal core is denoted by $\mathfrak{R}_\mathrm{G}$. When there are no windings on the block core, or when the winding on the block core is not connected, no MMF is generated in the block core. However, due to the existence of

the magnetic path, the reluctance of the block core and air gap exists in the equivalent magnetic circuit of a CM choke with an unconnected block core.

An equivalent circuit of the CM choke with different numbers of turns on the block core can be easily obtained from the equivalent magnetic circuit shown in Fig. 2. In the equivalent electrical circuit, the reluctances of the windings $\mathrm{T}_1\prime$, $\mathrm{T}_1\prime\prime$ are combined and represented by an inductance $L_{\mathrm{T}1}$ for simplification, while an inductance $L_{\mathrm{B}2}\prime$ symbolizes the reluctance of the block core $\mathfrak{R}_{\mathrm{B}2}\prime$. Therefore, $L_{\mathrm{T}1}$ and $L_{\mathrm{B}2}\prime$ together denote the first winding of the CM choke. Similarly, $L_{\mathrm{T}3}$ and $L_{\mathrm{B}2}$ characterize the second winding. The CM and DM configurations of the CM choke with a block core are shown in Figs. 2b and 2d, respectively. The inductance matrix is completely populated, with all non-zero mutual inductances; in Figs. 2b and 2d, couplings are shown only between neighboured windings to reduce complexity.

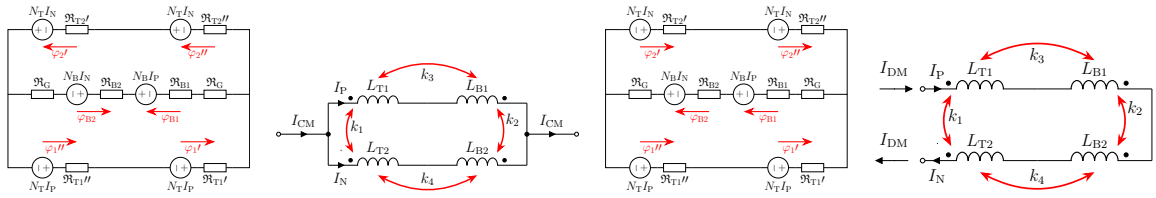

(a) Magnetic circuit (CM) (b) Electrical circuit (CM) (c) Magnetic circuit (DM) (d) Electrical circuit (DM)

Fig. 2. Magnetic and electrical circuits of single-phase CM choke with block core [5]

C. Common-Mode Inductance of the CM Chokes with a Block Core

The inductance of an inductor can be expressed in terms of the ratio of induced voltage to the rate of change of current.

$$L = \frac{V}{\frac{\mathrm{d}I}{\mathrm{d}t}} \tag{1}$$

In a single-phase system, the CM current flows in the same direction through the phase and neutral conductors and returns through the ground path. These equal currents create an equal voltage drop across both the phase conductor winding and the neutral conductor winding of the CM choke. The currents in the phase conductor and neutral conductor and the voltage in CM configurations can be expressed as follows:

$$I_{\mathrm{P\_Conv(CM)}} = I_{\mathrm{N\_Conv(CM)}} = \frac{I_\mathrm{CM}}{2} \tag{2a}$$

$$V_{\mathrm{P\_Conv(CM)}} = V_{\mathrm{N\_Conv(CM)}} = V_\mathrm{CM} \tag{2b}$$

The voltage drops across the phase and neutral windings can be written in the form of a matrix [5]

$$\begin{bmatrix} V_{\mathrm{P\_Conv}} \\ V_{\mathrm{N\_Conv}} \end{bmatrix} = \begin{bmatrix} L_{\mathrm{leakage\_1}} + \frac{N^2}{4\mathfrak{R}_\mathrm{T}} & \frac{N^2}{4\mathfrak{R}_\mathrm{T}} \\ \frac{N^2}{4\mathfrak{R}_\mathrm{T}} & L_{\mathrm{leakage\_2}} + \frac{N^2}{4\mathfrak{R}_\mathrm{T}} \end{bmatrix} \begin{bmatrix} \frac{\mathrm{d}I_{\mathrm{P\_Conv}}}{\mathrm{d}t} \\ \frac{\mathrm{d}I_{\mathrm{N\_Conv}}}{\mathrm{d}t} \end{bmatrix} \tag{3}$$

In this equation, $L_{\mathrm{leakage\_i}}$ denotes the leakage inductance of the ith winding, N is the number of turns on a toroidal core in a conventional CM choke, and $\mathfrak{R}_\mathrm{T}$ refers to the reluctance of a quadrant of the toroidal core and can be expressed using the following equation.

$$\mathfrak{R}_\mathrm{T} = \frac{\frac{l_{\mathrm{e\_T}}}{4}}{\mu_{\mathrm{r\_T}}\mu_0 A_{\mathrm{e\_T}}} \tag{4}$$

Here, $l_{\mathrm{e\_T}}$ and $A_{\mathrm{e\_T}}$ indicate the mean length and effective cross-section of the toroidal core, respectively, and can be expressed as follows:

$$A_{\mathrm{e\_T}} = (r_\mathrm{out} - r_\mathrm{in}) \cdot h \tag{5}$$

$$l_{\mathrm{e\_T}} = \frac{2\pi \cdot \ln\left(\frac{r_\mathrm{out}}{r_\mathrm{in}}\right)}{\frac{1}{r_\mathrm{in}} - \frac{1}{r_\mathrm{out}}} \tag{6}$$

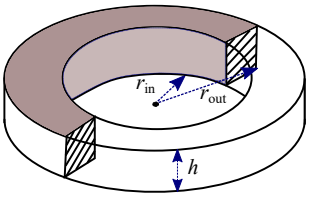

Fig. 3. Toroidal core

Here, r_in, r_out denote the inner and outer radii of the core, respectively, and h is the height of the toroidal core.

Using Equations (1), (2) and (3), the CM inductance of a conventional CM choke can be expressed as follows:

$$L_{\mathrm{CM\_Conv}} = \frac{L_{\mathrm{leakage\_1}}}{2} + \frac{N^2}{4\mathfrak{R}_\mathrm{T}} \cong \frac{N^2}{4\mathfrak{R}_\mathrm{T}} \tag{7}$$

In the equivalent equation for the CM inductance written above, the leakage inductance part was ignored because the leakage inductance does not affect the CM inductance significantly. Using the CM inductance of a

conventional CM choke from Equation (7), the CM inductance of a single-phase CM choke with a block core can be expressed as follows [5]:

$$L_{\mathrm{CM\_New}} \cong \frac{L_{\mathrm{leakage\_1}\prime} + L_{\mathrm{leakage\_1}\prime\prime} + L_{\mathrm{leakage\_B1}}}{2} + \frac{N^2}{\mathfrak{R}_{\mathrm{T}}} \cong \frac{N_{\mathrm{T}}^2}{\mathfrak{R}_{\mathrm{T}}} \tag{8}$$

Here, $L_{\mathrm{leakage\_1}\prime}$, $L_{\mathrm{leakage\_1}\prime\prime}$ and $L_{\mathrm{leakage\_B1}}$ are together considered as the leakage inductance of a winding, since $\mathrm{T}_1\prime$, $\mathrm{T}_1\prime\prime$ and B_1 comprise a single winding of this choke. When calculating the CM inductance, these leakage parts are ignored because the fluxes in the block core cancel each other out. Comparing Equations (8) and (7), it can be seen that $L_{\mathrm{CM\_Conv}} = L_{\mathrm{CM\_New}}$ when $N_{\mathrm{T}} = \frac{N}{2}$, where N is the number of turns in each winding of the conventional CM choke and N_{T} denotes the number of turns in each winding of the new-design choke.

D. Differential-Mode Inductance of the CM Choke with a Block Core

Since the DM current flows through the phase conductor and the neutral conductor in opposite directions in a single-phase system, the phase and neutral currents and voltage can be expressed as follows:

$$I_{\mathrm{P\_Conv(DM)}} = -I_{\mathrm{N\_Conv(DM)}} = I_{\mathrm{DM}} \tag{9a}$$

$$V_{\mathrm{P\_Conv(DM)}} = -V_{\mathrm{N\_Conv(DM)}} = V_{\mathrm{DM}} \tag{9b}$$

The DM inductance of a conventional single-phase CM choke can be expressed using Equations (1), (9) and (3)

$$L_{\mathrm{DM\_Conv}} \cong L_{\mathrm{leakage\_1}} \tag{10}$$

In this equation, $\frac{N^2}{4\mathfrak{R}_{\mathrm{T}}}$ is ignored because only leakage inductance is considered in the calculation of DM inductance. The leakage inductance mainly depends on the air gap inside the toroidal core and the core geometry. The leakage inductance of a CM choke can be calculated using the following equation [1],

$$L_{\mathrm{leakage}} \cong 2.5\mu_0 N_{\mathrm{T}}^2 \frac{A_{\mathrm{e}}}{l_{\mathrm{eff}}} \left(\frac{l_{\mathrm{e}}}{2} \sqrt{\frac{\pi}{A_{\mathrm{e}}}} \right)^{1.45} \tag{11}$$

Here, l_{eff} is the mean effective path length of the leakage flux and can be calculated from Equation (12). Here, d_{in}, d_{out} denote the inner and outer diameters of the toroidal core, respectively, and θ is the angle of the adjacent turns of the winding due to the curvature of the toroid [1].

$$l_{\mathrm{eff}} = \sqrt{\frac{{d_{\mathrm{out}}}^2}{\sqrt{2}} \left(\frac{\theta}{4} + 1 + \sin\frac{\theta}{2} \right) + {d_{\mathrm{in}}}^2 \left(\frac{\theta}{4} - 1 + \sin\frac{\theta}{2} \right)} \tag{12}$$

Since the leakage inductance of a single winding in this new-design CM choke with a block core consists of the contributions of three windings, it can be stated as follows [5]:

$$L_{\mathrm{DM\_New}} \cong L_{\mathrm{leakage\_1}\prime} + L_{\mathrm{leakage\_1}\prime\prime} + L_{\mathrm{leakage\_B1}} + \frac{2(N_{\mathrm{B}} + N_{\mathrm{T}})^2}{\mathfrak{R}_{\mathrm{C}}} \tag{13}$$

The additional factor accounts for the number of turns on the block core which aid in increasing the DM inductance of the structure. Usually, the leakage inductance of the winding on the block core $L_{\mathrm{leakage\_B1}}$ is lower than the leakage inductance of the winding on the toroidal core. The reason for this is that the number of turns in the winding on the block core is lower. A lower number of turns is usually wound on the block core to avoid early core saturation. Since the two windings on the toroidal core count as a single winding, the equation written above can be simplified so that $L_{\mathrm{leakage\_1}\prime} + L_{\mathrm{leakage\_1}\prime\prime} + L_{\mathrm{leakage\_B1}}$ is approximately equal to $2L_{\mathrm{leakage}}$. In addition, the leakage inductance of the winding on the block core is negligible because its value is much smaller than the leakage inductance of the winding on the toroidal core. Therefore, Equation (13) can be expressed as follows [5]:

$$\begin{aligned} L_{\mathrm{DM\_New}} &\cong 2L_{\mathrm{leakage}} + \frac{2(N_{\mathrm{B}} + N_{\mathrm{T}})^2}{\mathfrak{R}_{\mathrm{C}}} \\ &\cong 5\mu_0 N_{\mathrm{T}}^2 \frac{A_{\mathrm{e}}}{l_{\mathrm{eff}}} \left(\frac{l_{\mathrm{e}}}{2} \sqrt{\frac{\pi}{A_{\mathrm{e}}}} \right)^{1.45} + \frac{2(N_{\mathrm{B}} + N_{\mathrm{T}})^2}{\mathfrak{R}_{\mathrm{C}}} \end{aligned} \tag{14}$$

In this equation, N_{B} and N_{T} indicate the number of turns in each winding on the block core and the toroidal core, respectively. The total reluctance of the toroidal core and block core combined is denoted by $\mathfrak{R}_{\mathrm{C}}$, which can be expressed as follows:

$$\mathfrak{R}_{\mathrm{C}} = 2\mathfrak{R}_{\mathrm{B}} + 2\mathfrak{R}_{\mathrm{G}} + \mathfrak{R}_{\mathrm{T}} \tag{15}$$

In this equation, $\mathfrak{R}_{\mathrm{B}}$ represents the reluctance of either half of the block core and $\mathfrak{R}_{\mathrm{G}}$ represents the reluctance of the air gap, where

$$\mathfrak{R}_{\mathrm{B}} = \frac{l_{\mathrm{e\_B}}}{\mu_{\mathrm{r\_B}}\mu_0 A_{\mathrm{e\_B}}} \text{ and } \mathfrak{R}_{\mathrm{G}} = \frac{l_{\mathrm{e\_G}}}{\mu_0 A_{\mathrm{e\_G}}} \tag{16}$$

In the above equations, $\mu_{\mathrm{r\_B}}$, $l_{\mathrm{e\_B}}$, and $A_{\mathrm{e\_B}}$ denote the the relative permeability, effective path length, and effective cross-section of the block core, respectively.

III. Other Parameters of CM Choke with Block Core

A. Effect of the Number of Turns on the Block Core on the CM and DM Attenuation

To investigate the influence of the number of turns on the block core, we have performed an investigation with different numbers of turns on the block core (L = 23.8 mm, W = 5 mm, H = 12.5 mm) and a fixed number of turns of 13 in each winding on the toroidal core (d_{out} = 41.8 mm, d_{in} = 26.2 mm, h = 12.5 mm). Since $N_{\mathrm{T}} = \frac{N}{2}$ is applicable, the attenuation of this CM choke with a block core is compared with a conventional CM choke with 26 turns. Fig. 4 shows a comparison of the DM inductance between the conventional CM choke and the CM choke with a block core. The relative permeability of the ferrite block core is $\mu_{\mathrm{r\_B}}$ =2200, and the relative permeability of the ferrite toroidal core is $\mu_{\mathrm{r\_T}}$ = 4300. When a block core without turns is inserted into the air gap of the toroid, the DM inductance of the CM choke increases significantly, as mentioned in Tab. I. This unconnected block core could act as a shield to minimize the coupling between two windings on the toroidal core and results in a higher leakage or DM inductance. A comparison between the analytical and measured CM and DM inductance values is shown in Tab. I. The analytical values of the CM and DM inductance are very similar to the measured values, which confirms the correctness of the analytical formula for calculating the inductance of a CM choke with a block core.

As the number of turns on the block core increases, the DM inductance also increases, as shown in Fig. 4a. The effect of the increasing number of turns can be seen in the DM attenuation curves, as shown in Fig. 4b. However, as the number of turns on the block core increases, the winding resistance also increases. This winding resistance and the core loss of the block core also influence the total loss of the CM choke, which was not observed before in the investigation of the DM attenuation when the block core was unconnected. Moreover, when the block core is connected to the winding on the toroidal via different numbers of turns, the losses in the air gap between the toroid and the block core must also be taken into account, because the air gap also contributes to the total losses. To achieve optimum DM attenuation, it would make sense to use a block core without turns or with a low number of turns.

Figs. 4c and 4d show a comparison of the CM inductance and CM attenuation of the conventional CM choke and the single-phase CM choke with different numbers of turns on the block core. No substantial effect can be observed in the CM inductance and CM attenuation of a CM choke with different numbers of turns on the block core because the opposite winding direction on the block core mutually balances the magnetic fluxes for the CM current.

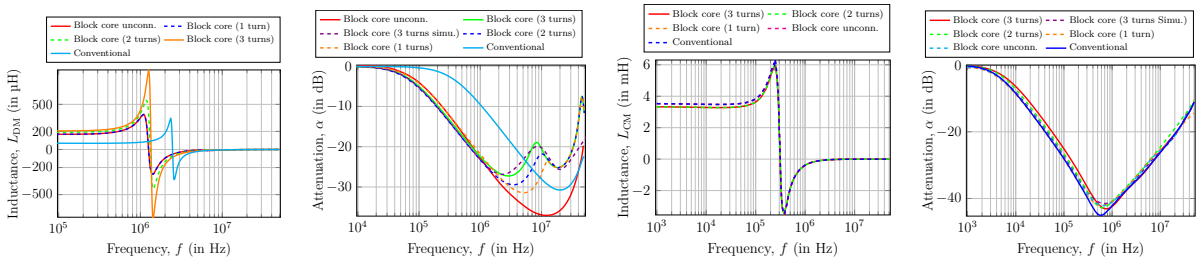

(a) Measured DM inductance (b) DM attenuation (c) Measured CM inductance (d) CM attenuation

Fig. 4. A common-mode choke with a block core; (a, c) Measured DM and CM inductance; (b, d) Measured and simulated DM and CM attenuation

TABLE I
CM AND DM INDUCTANCE OF THE FERRITE CM CHOKE WITH THE FERRITE BLOCK CORE

Structure	N_{T}	N_{B}	CM inductance, L_{CM}		DM inductance, L_{DM}		
			Analytical	Measured	Analytical	Measured	% of increased L_{DM} from conventional L_{DM} (measured)
Conventional	$N = 26$	-	3.5 mH (7)	3.7 mH	67.8 µH (11)	69.381 µH	-
Unconnected block core	$N = 26$	-	3.5 mH (7)	3.7 mH	170.9 µH (14)	171.13 µH	146.89 %
Connected block core	13	1	3.5 mH (7)	3.7 mH	175.2 µH (14)	173.15 µH	149.56 %
Connected block core	13	2	3.5 mH (7)	3.6 mH	190.22 µH (14)	193.70 µH	179.183 %
Connected block core	13	3	3.5 mH (7)	3.6 mH	202.33 µH (14)	207.54 µH	199.131 %

B. Effect of the Air-Gap Length on the Single-Phase CM Choke with a Block Core

As the air gap is a high impact in the modified CM choke, the influence of the air gap is investigated for two distinct air gap lengths, $0.5\,\mathrm{mm}$ and $0.7\,\mathrm{mm}$, as shown in Figs. 5 (a, b). The increased reluctance reduces the total DM inductance of the circuit, as shown in Tab. II.

The simulated CM and DM inductances are obtained by using the simulation model in ANSYS Q3D and the CM and DM inductances of the simulated model can be obtained using the following equations [11]: $L_{\mathrm{CM}} = \frac{L+M}{2}$, $L_{\mathrm{DM}} = 2(L-M)$. Here, L is the self-inductance of a winding and M is the mutual inductance between the windings. In Tab. II, it can be seen that the numerical results are in a good agreement with the analytical and measurement results.

(a) Air-gap length = $0.45\,\mathrm{mm}$ (b) Air-gap length = $0.7\,\mathrm{mm}$

Fig. 5. A CM choke with a block core (a) Simulation model with the air-gap length, $l_{\mathrm{e\_G}}$ = $0.5\,\mathrm{mm}$ (b) Simulation model with the air-gap length, $l_{\mathrm{e\_G}}$ = $0.7\,\mathrm{mm}$

TABLE II
CM AND DM INDUCTANCES FOR DIFFERENT LENGTHS OF AIR GAP BETWEEN CM CHOKE AND BLOCK CORE

Length of air gap, $l_{\mathrm{e\_G}}$	N_{T}	N_{B}	CM inductance, L_{CM}			DM inductance, L_{DM}		
			Measured	Analytical	Simulated	Measured	Analytical	Simulated
$0.5\,\mathrm{mm}$	13	3	$3.6\,\mathrm{mH}$	$3.48\,\mathrm{mH}$ (7)	$3.5\,\mathrm{mH}$	$207.54\,\mu\mathrm{H}$	$202.33\,\mu\mathrm{H}$ (14)	$201.65\,\mu\mathrm{H}$
$0.7\,\mathrm{mm}$	13	3	$3.6\,\mathrm{mH}$	$3.48\,\mathrm{mH}$ (7)	$3.5\,\mathrm{mH}$	$204.68\,\mu\mathrm{H}$	$197.81\,\mu\mathrm{H}$ (14)	$198.88\,\mu\mathrm{H}$

C. Influence of the Relative Permeability of the Toroidal Core on Improvement of the DM Inductance

The relative permeability of the core plays one of the most important roles in achieving the required inductance. Two toroidal cores with the same dimensions but with different relative permeabilities of 2200 and 4300 are chosen to observe the effect on DM inductance when the permeability of the toroidal core varies. The block core's relative permeability is kept constant at 2200. When the relative permeability is the same for the block core and toroidal core, the improvement in the DM inductance after the block core is placed in the toroidal core is almost $56\,\%$ higher than for the high-permeability toroidal core, as shown in Fig. 6a and Tab. III.

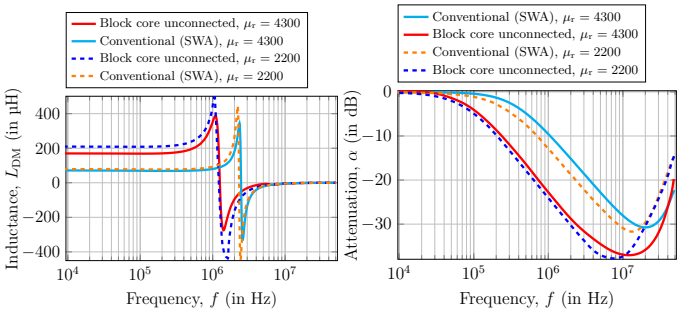

(a) Measured DM inductance (b) Measured DM attenuation

Fig. 6. Comparison of the DM attenuation and DM inductance of two single-phase CM chokes with a ferrite core of different relative permeability and with an unconnected winding on the block core. Here, SWA refers to the small winding angle between two adjacent turns in each winding on the toroidal core (see Fig. 1)

TABLE III
COMPARISON OF THE MEASURED CM AND DM INDUCTANCES OF CM CHOKE MADE WITH A FERRITE CORE OF DIFFERENT RELATIVE PERMEABILITY AND WITH AN UNCONNECTED BLOCK CORE

μ_{r} of ferrite core	N	CM inductance, L_{CM}	DM inductance, L_{DM}		% of increase of L_{DM}
			Conventional	Block core	
$\mu_{\mathrm{r}} = 4300$	26	$3.8\,\mathrm{mH}$	$67.8\,\mu\mathrm{H}$	$171.13\,\mu\mathrm{H}$ (14)	$135.71\,\%$
$\mu_{\mathrm{r}} = 2200$	26	$1.7\,\mathrm{mH}$	$72.3\,\mu\mathrm{H}$	$210.9\,\mu\mathrm{H}$ (14)	$191.70\,\%$

D. Effect of Different Materials for the Toroidal Core and Block Core

This section contains a brief discussion about the performance of the newly proposed CM choke when the materials used for the toroidal core and block core are different. For this purpose, a nanocrystalline toroidal core and a ferrite block core are used. The block core's placement in the nanocrystalline choke also increases its DM inductance, which rises further in parallel with the numbers of turns. Tab. IV shows a comparison between the inductances of the unconnected block core in the conventional CM choke with a ferrite core and in the conventional CM choke with a nanocrystalline core. The rise in the DM inductance of the CM choke with a nanocrystalline core is somewhat lower compared to the conventional CM choke with a ferrite core. Due to the high permeability of the CM choke with a nanocrystalline core, more flux linkage and less leakage occur in the inner air gap, resulting in a higher coupling coefficient than for the choke with a ferrite core. Therefore, the rate of increase of the DM inductance in the CM choke with a nanocrystalline core and a ferrite block core is low. A nanocrystalline block core in the CM choke with a nanocrystalline core increases the DM inductance as expected. Including the block core in the CM choke with a nanocrystalline toroidal core improves the DM attenuation and shifts the DM self-resonance, both at low frequencies, as shown in Fig. 7c. Further increasing

the number of turns on the block core improves the attenuation at low frequencies below the resonant frequency. However, above the resonant frequency, the attenuation is degraded. Since block core made with a ferrite has larger losses than the CM choke with a nanocrystalline core, the losses from the block core may dominate here, worsening the high-frequency attenuation.

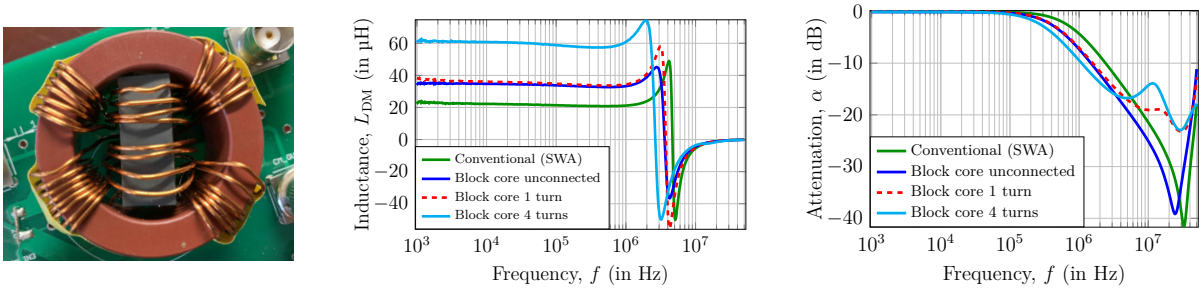

(a) Physical module (b) Measured DM inductance (c) Measured DM attenuation

Fig. 7. Nanocrystalline CM choke with 4 turns on block core: (a) Physical module; (b, c) Comparison of the measured DM inductance and DM attenuation of the CM choke with a nanocrystalline toroidal core with different numbers of turns on the ferrite block core

TABLE IV
COMPARISON OF MEASURED CM AND DM INDUCTANCES OF CM CHOKES (FERRITE AND NANOCRYSTALLINE TOROIDAL CORES) WITH AN UNCONNECTED FERRITE BLOCK CORE

Core type	N	CM inductance	DM inductance, L_{DM}		% of increase of L_{DM}
			Conventional	Block core	
Ferrite	26	3.8 mH	67.8 µH	171.13 µH	135.71 %
Nanocrystalline	14	12 mH	21.8 µH	35.9 µH	64.67 %

E. Core Saturation Analysis

Though it is considered that a high DM current and the associated leakage fluxes are the main reasons for the core saturation of a CM choke, the magnetic flux produced by the CM current can also cause the core saturation. Therefore, both CM and DM currents, and the associated CM and DM magnetic flux densities must be considered when analyzing core saturation. To investigate the core saturation of a CM choke using the CM and DM currents, we have conducted a measurement with the DPG10 1500B power choke tester. Fig. 8a shows a comparison of the DM saturation current for different winding strategies of the CM choke built with a ferrite core. As the leakage or DM inductance of the CM choke increases with different winding strategies, it can be seen that the core starts to saturate at a smaller current. However, the CM choke with a nanocrystalline core shows better performance than the choke with a ferrite core in the DM core saturation analysis, as shown in Fig. 8b. The nanocrystalline core has higher saturation flux density and smaller leakage inductance due to the high permeability and high coupling between windings. The ferrite block core with 4 turns in the CM choke with a nanocrystalline toroidal core provides higher DM inductance than the other configurations of the CM choke with a nanocrystalline core up to 35 A, and then starts to decrease. Therefore, it can be concluded that when improving the DM inductance, the number of turns on the block core must be carefully selected. In addition, when the DM current is high, it is better to choose a nanocrystalline core to avoid DM saturation of the core. The CM current that flows through a circuit is usually smaller than the DM current. Figs. 8c and 8d also verify that for both cores, the CM core saturation behavior of the choke with a block core is the same as the conventional CM choke without a block core.

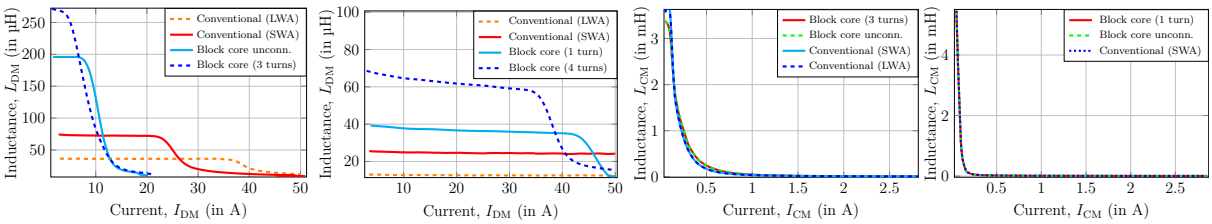

(a) Ferrite (DM) (μ_r = 4300, SWA) (b) Nanocrystalline (DM) (c) Ferrite (CM) (d) Nanocrystalline (CM)

Fig. 8. Comparison of the incremental inductance versus saturation current: (a) Ferrite CM choke (DM configuration); (b) Nanocrystalline CM choke (DM configuration); (c) Ferrite CM choke (CM configuration); (d) Nanocrystalline CM choke (CM configuration). Here, SWA and LWA mean small and large winding angles.

III. Performance of the CM Choke with a Block Core in an EMI Filter

To evaluate the performance in attenuating EMI noise, we inserted the CM choke with the block core into a ready built EMI filter. Fig. 9a shows the existing EMI filter, which is used to compare different winding strategies for a CM choke on the same PCB and under the same conditions. This filter works as a CLCL

topology in the DM configuration and as an LCL topology in the CM configuration. Fig. 9d shows the equivalent electrical circuit diagram of the existing EMI filter. The magenta box in the circuit indicates where the first CM inductor is replaced for these measurements. Figs. 9b and 9e show that there is no significant difference in the CM attenuation of the EMI filter with the conventional CM choke and alternatively with the choke with the unconnected block core. Furthermore, it also proves that an increase in the number of turns on the block core does not have any remarkable effect on the CM attenuation of the filter. The DM attenuation of the filter shown in Figs. 9c and 9f indicates that the insertion of the block core serves its purpose quite well. Fig. 9c shows that for the ferrite choke with block core (3 turns), the first resonant frequency shifted to 6 kHz from 11 kHz. In addition, approximately 15 dB to 17 dB more attenuation can be achieved at the lower frequencies using a CM choke with a ferrite core (with 3 turns on the block core). Using the nanocrystalline CM choke with 4 turns on the block core, as shown in Fig. 9f, about 10 dB to 12 dB more attenuation can be obtained than when using the conventional CM choke, without any significant change in the high-frequency performance.

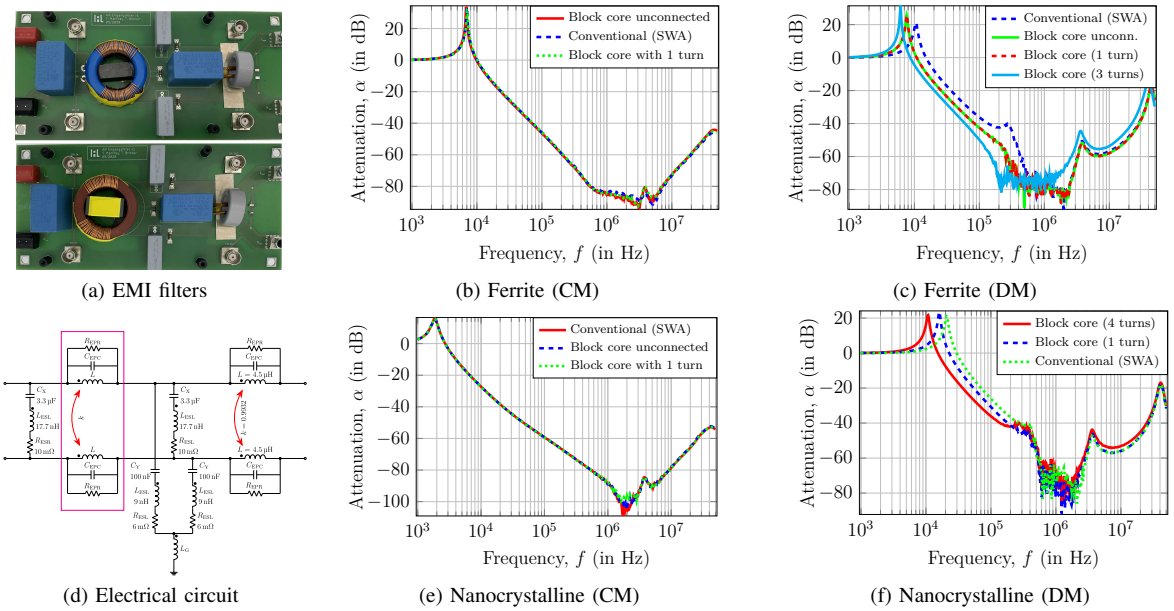

(a) EMI filters (b) Ferrite (CM) (c) Ferrite (DM)

(d) Electrical circuit (e) Nanocrystalline (CM) (f) Nanocrystalline (DM)

Fig. 9. Measurement of different CM chokes using an existing EMI filter: (a) EMI filter with the CM choke (made with ferrite and nanocrystalline cores + the ferrite block core); (b, e) Comparison of the CM attenuation with the conventional CM choke (made with a ferrite core) and the CM choke with a nanocrystalline core (with block core made from ferrite) in the existing EMI filter; (c, f) Comparison of the DM attenuation with the conventional CM choke (made from ferrite) and the CM choke with a nanocrystalline core (with block core made from ferrite) in the existing EMI filter; (d) An equivalent electrical circuit diagram of the existing EMI filter

IV. Possible Structure of a Three-Phase CM Choke with Integrated DM Inductance

For a three-phase CM choke, the block core must be Y-shaped to fit between the three windings of the conventional three-phase CM choke. The three legs of the Y-core should be spaced 120° apart to ensure symmetry. This newly proposed choke consists of six copper windings on the toroidal core and three on the Y-core, as shown in Fig. 10a. To maintain the symmetrical structure and symmetrical coupling between the windings, the six windings on the toroidal core must have an identical number of turns. The installation of a Y-core directly increases the leakage inductance by reducing the coupling between the windings.

A. Magnetic Flux Direction in a Three-Phase CM Choke with a Y-Core

The three-phase CM choke with Y-core works in the same way as the single-phase CM choke with block core, except that it has nine windings instead of six. The magnetic flux directions of the CM and DM configurations of this newly proposed three-phase choke are mentioned in Figs. 10b and 10c, respectively. In these figures, the violet, blue and green arrows denote the currents for phases U, V, W, respectively, and red arrows indicate the flux direction. As shown in Fig. 10b, the flux induced by the CM current is oriented anti-clockwise, and for the two windings on the toroid, the fluxes add to attenuate the CM noise. As seen in the single-phase CM choke with the block core, the induced fluxes in the Y-core also cancel each other out in the CM configuration, without affecting the CM performance of the three-phase CM choke. In contrast, in the DM configuration, the magnetic fluxes in the Y-core help to create magnetic paths through the air gap of the three-phase choke, as shown in Fig. 10c, thereby leading to more leakage flux and more DM inductance. However, fluxes φ_{B2} and φ_3 are in the opposite direction and can offset some of the flux, weakening the magnetic path through winding B2 for flux φ_3. Nevertheless, the other two windings on the Y-core help minimize this problem by keeping the magnetic path intact and providing the expected DM inductance.

B. Magnetic and Electrical Circuits of a Three-Phase CM Choke with a Y-Core

Based on the magnetic circuit discussed in Section (II-B), the CM and DM magnetic circuits are drawn in Figs. 11a and 11c for the three-phase CM choke with a Y-core, respectively. In the CM configuration, as shown in Fig. 11a, the induced fluxes φ_1, φ_1'', φ_2, φ_2'', φ_3, and φ_3'' in the toroidal core sum up to eliminate the CM noise. Furthermore, the induced fluxes φ_{B1}, φ_{B2}, and φ_{B3} in the Y-core cancel each other out without affecting the CM inductance of the choke. In the DM configuration shown in Fig. 11c, the fluxes φ_2, φ_2'', φ_3, and φ_3'' add up. But most of these fluxes are canceled out when they encounter the fluxes φ_1, φ_1'', and the fluxes that are not canceled out generate some leakage flux. However, as shown in Fig. 11c, the fluxes φ_{B1}, φ_{B2}, and φ_{B1}, φ_{B3} establish magnetic paths through the air gap for the leakage flux of the windings T_1, T_1'', T_2 and T_2''. These leakage fluxes improve the DM inductance. As discussed in Section (II-B) an equivalent electrical circuit for the three-phase CM choke with different numbers of turns on the Y-core can be easily obtained from the equivalent magnetic circuit shown in Fig. 11.

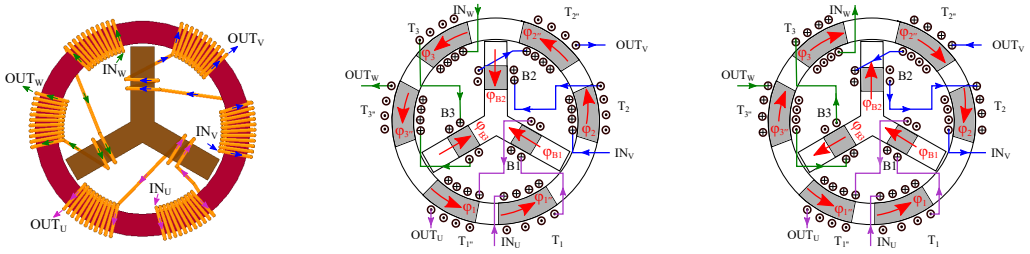

(a) Y-core with 2 turns (b) CM flux direction (c) DM flux direction

Fig. 10. Three-phase CM choke with a Y-core: (a) Simulation model of the three-phase CM choke with a Y-core; (b) CM flux direction; (c) DM flux direction

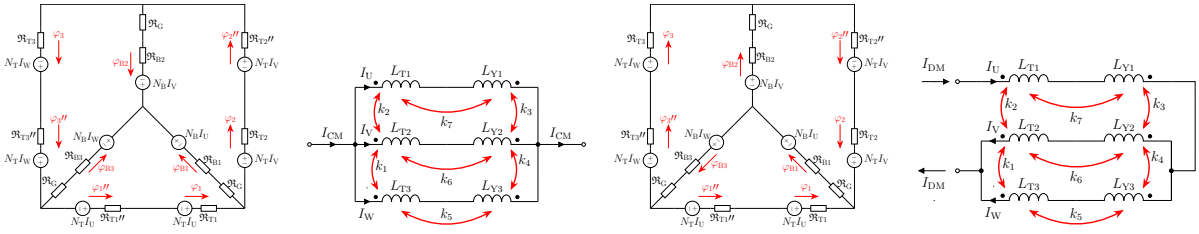

(a) Magnetic circuit (CM) (b) Electrical circuit (CM) (c) Magnetic circuit (DM) (d) Electrical circuit (DM)

Fig. 11. Magnetic and electrical circuits for the three-phase CM choke with a Y-core

C. CM and DM Inductance of a Three-Phase Common-Mode Choke with a Y-core

The three-phase CM choke with the Y-core model shown in Fig. 10a is simulated in ANSYS Q3D to extract the self-inductance of the each winding and obtain the coupling between the windings. As with the newly designed single-phase choke $N_T = \frac{N}{2}$, which is discussed in Section (II-C), the newly proposed three-phase choke is built with 11 turns in each winding to fairly compare it with the conventional choke with 22 turns. Then the total DM and CM inductances of the choke using the extracted parameters from the 3D-FEM simulation model are obtained using Equations (9) and (10) as proposed in [7], respectively. Subsequently, to verify the simulated CM and DM inductances, the analytical values of the CM and DM inductances are calculated using Equations (8) and (14). The equations used for a single-phase CM choke also apply to the three-phase CM choke with a Y-core since each winding of the choke comprises two windings on the toroidal core and one winding on the Y-core. This winding structure is similar to that of the single-phase CM choke with a block core, and the only change is in the calculation of the total reluctance of the choke. In the three-phase CM choke with a Y-core, the Y-core consists of three parts, and there are three air gaps active between the toroid and the Y-core. Therefore, the total reluctance of this newly proposed choke can be expressed as follows:

$$\mathfrak{R}_C = 3\mathfrak{R}_B + 3\mathfrak{R}_G + \mathfrak{R}_T \tag{17}$$

A comparison between the analytical and simulated CM and DM inductances of the conventional three-phase CM choke and the three-phase CM choke with the Y-core is provided in Table V.

TABLE V
COMPARISON OF THE ANALYTICAL AND SIMULATED CM AND DM INDUCTANCES OF A CONVENTIONAL THREE-PHASE CM CHOKE AND THREE-PHASE CM CHOKE WITH A Y-CORE

Inductance	Conventional (N=22)		With Y-core (N_B=2, N_T=11)	
	Analytical	Simulation	Analytical	Simulation
k		0.9964		0.9931
CM inductance, L_{CM}	8.2 mH (7)	8.22 mH	8.2 mH (7)	8.16 mH
DM inductance, L_{DM}	43.79 µH (11)	44.02 µH	83.51 µH (14)	83.64 µH

When calculating the analytical DM inductance of the newly proposed choke, Equation (17) supplies the value of $\mathfrak{R}_C$ in Equation (14).

V. Performance of the Three-Phase CM Choke with a Y-core in a Filter

To investigate the performance of a three-phase CM choke with a Y-core in an EMI filter, we performed a simulation in ANSYS circuit simulator because the actual physical Y-core is not readily available on the market. The physical filter and the schematic diagram of the electrical circuit of the three-phase EMI filter are shown in Fig. 12a and Fig. 12b, respectively. In the beginning, the simulation results are validated using the measurement results from a conventional three-phase CM choke in a three-phase EMI filter, as shown in Fig. 12a. Fig. 12c shows that a Y-core in a three-phase CM choke does not affect the CM attenuation of the EMI filter, as with the block core in the single-phase CM choke. Nevertheless, the simulation result shown in Fig. 12d indicates that this newly proposed three-phase CM choke will also improve the DM attenuation of the EMI filter. So, it can be summarized that a three-phase CM choke with a Y-core could be an exciting new choice for a three-phase EMI filter.

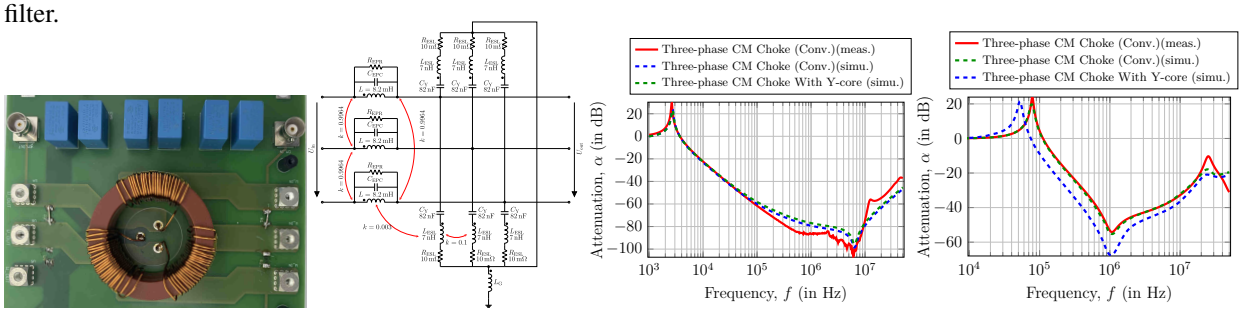

(a) Three-phase EMI filter (b) Electrical circuit (c) CM attenuation (d) DM attenuation

Fig. 12. (a) Conventional three-phase CM choke in the three-phase EMI filter; (b) Circuit diagram of the electrical circuit of the three-phase EMI filter; (c, d) Measured and simulated CM and DM attenuation of the three-phase conventional CM choke and the three-phase CM choke with a Y-core

VI. Conclusion

A purpose-built common-mode choke designed well for the application is essential to achieve the desired attenuation from an EMI filter. To improve the DM inductance of a single-phase choke, the authors of [5] have proposed a CM choke with an integrated DM inductance, created with an additional block core. This configuration has been analyzed, designed and tested, and the performance has been evaluated as a standalone component and integrated into an EMI filter. The concept successfully increases the DM inductance up to a certain DM saturation current. Different core materials have been evaluated. It has been shown that the CM choke with a nanocrystalline core shows better performance than the choke with a ferrite core in the DM core saturation analysis. The DM attenuation of an EMI filter can be improved this way, until the core saturates. The numerical and experimental analysis of different parameters that affect the performance of the newly proposed choke has been discussed. It was noted that the numerical results are in a good agreement with the analytical and measurement results. Moreover, a proposal for a three-phase CM choke has been made. Its magnetic flux distribution, magnetic circuit and electrical circuit have been explained and discussed in this paper. The performance of a three-phase EMI filter with a three-phase CM choke incorporating a Y-core has also been discussed.

References

[1] M.J. Nave, “On modeling the common mode inductor,” *in IEEE International Symposium on Electromagnetic Compatibility*, 1991.

[2] L. Dehong, J. Xanguo, "High frequency model of common mode inductor for EMI analysis based on measurements," *in 3rd International Symposium on Electromagnetic Compatibility,* 2002.

[3] K. Kostov and J. Kyyra, "Common-mode choke coils characterization," *in 13th European Conference on Power Electronics and Applications,* 2009.

[4] A. Massarini, M. K. Kazimierczuk and G. Grandi, "Lumped parameter models for single- and multiple-layer inductors," *in PESC Record. 27th Annual IEEE Power Electronics Specialists Conference,* 1996.

[5] J. Borsalani, A. Dastfan, J. Ghalibafan, “An Integrated EMI Choke With Improved DM Inductance,” *in IEEE Transactions on Power Electronics*, 2021.

[6] Fang Luo, Dushan Boroyevich, Paolo Mattevelli, Khai Ngo, David Gilham and Nicolas Gazel “An integrated common mode and differential mode choke for EMI suppression using magnetic epoxy mixture,” *The 26th Annual IEEE Applied Power Electronics Conference and Exposition (APEC)*, 2011.

[7] M. Ali, T. Brinker, J. Friebe, A. Mertens, “Analysis of EMI Filter Attenuation under the Influence of Parasitic Elements of Components and their Mutual Couplings,” *The 23rd European Conf. on Power Electronics and Applications (ECCE Europe 2021)*, September 2021.

[8] M. Ali, J. Friebe, A. Mertens, “Design and Optimization of Input and Output EMI Filters under the Influence of Parasitic Couplings,” *The 23rd European Conf. on Power Electronics and Applications (ECCE Europe 2021)*, September 2021.

[9] H. Kim et al., "A new asymmetrical winding common mode choke capable of attenuating differential mode noise," *in 8th International Conference on Power Electronics - ECCE Asia*, 2011.

[10] D. Xu, C. K. Lee, S. Kiratipongvoot and W. M. Ng, "An Active EMI Choke for Both Common- and Differential-Mode Noise Suppression," *in IEEE Transactions on Industrial Electronics*, vol. 65, no. 6, pp. 4640-4649, June 2018, doi: 10.1109/TIE.2017.2764859.

[11] M. Ali, J. Friebe, A. Mertens, “Simplified Calculation of Parasitic Elements and Mutual Couplings of Wide-bandgap Power Semiconductor Modules,” *in European Conference on Power Electronics and Applications (EPE’20 ECCE Europe)*, 2020.